Lipids (2013) 48:197–207
DOI 10.1007/s11745-012-3739-1

METHODS

Stereoselective Synthesis and NMR Characterization of C-24 Epimeric Pairs of 24-Alkyl Oxysterols

Shoujiro Ogawa · Hiroaki Kawamoto · Takashi Mitsuma · Hiroki Fujimori · Tatsuya Higashi · Takashi Iida

Received: 24 August 2012 / Accepted: 22 October 2012 / Published online: 30 November 2012

Abstract Two pairs of C-24 epimeric (24*R*)-/(24*S*)-24-hydroxy-24-methyl-5α-cholestan-3*β*-yl acetates and (24*R*)-/(24*S*)-25-hydroxy-24-methyl-5α-cholestan-3*β*-yl acetates as well as some related 24-ethyl oxysterol analogs were stereoselectively synthesized directly from the respective parent 24-alkyl sterols by a remote *O*-insertion reaction with 2,6-dichloropyridine *N*-oxide (DCP) in the presence of a catalytic amount of (5,10,15,20-tetramesitylporphrinate) ruthenium(II) carbonyl complex [Ru(TMP)CO] and HBr. ^{1}H- and ^{13}C-NMR signals serving to differentiate each of the two epimeric pairs were interpreted. The C-24 alkyl oxysterols epimeric at C-24 were found to be effectively characterized by the aromatic solvent-induced shift (ASIS) by C_5D_5N, particularly for the difference in the ^{13}C resonances in the substituted cholestane side chain. A method for differentiating the ^{1}H and ^{13}C signal assignment of the terminal 26-/27-CH_3 in the *iso*-octane side chain was also discussed on the basis of a combined use of the preferred conformational analysis and HMQC and HMBC techniques. The present method may be useful for determining the stereochemical configuration at C-24 of this type of 24-alkyl oxysterols.

Keywords Alkylsterol · Oxysterol · 24-Hydroxylation · 25-Hydroxylation · (24*R*)-/(24*S*)-Epimer · ^{1}H NMR · ^{13}C NMR · Aromatic solvent-induced shift by C_5D_5N

S. Ogawa · T. Higashi
Faculty of Pharmaceutical Sciences, Tokyo University of Science, Noda, Chiba 278-8510, Japan

H. Kawamoto · T. Mitsuma · H. Fujimori · T. Iida (✉)
Department of Chemistry, College of Humanities and Sciences, Nihon University, Sakurajousui, Setagaya, Tokyo 156-8550, Japan
e-mail: takaiida@chs.nihon-u.ac.jp

Abbreviations

ASIS	Aromatic solvent-induced shift
LIS	Lanthanide-induced shift
NMR	Nuclear magnetic resonance
HMQC	Heteronuclear multiple quantum coherence
HMBC	Heteronuclear multiple bond correlation
DEPT	Distortionless enhancement by polarization transfer
HR	High resolution
ESI	Electrospray ionization
MS	Mass spectrometry

Introduction

Cholesterol is biosynthesized in the liver of mammals including humans and then transformed into various steroid hormones and bile acids. Phytosterols (e.g., campesterol, stigmasterol, and *β*-sitosterol) are cholesterol-like naturally occurring steroids found in many plants [1]. They block the absorption of cholesterol in the small intestines and can help lower the level of serum cholesterol and reduce the risk of heart disease [2]. Ergosterol (provitamin D_2) and its analogs, which are components of fungal cell membranes, do not belong to phytosterols, but their chemical structures are also very similar to phytosterols. These steroids in biological materials are all classified into the category of so-called "sterols", because their chemical structures vary only in the presence or absence of an alkyl group and/or a double bond in the C_{27} parent cholestane structure.

Meanwhile, oxysterols are defined as the oxygenated derivatives of sterols having additional hydroxy and/or oxo groups. In human, oxysterols have a remarkably diverse

profile of biological activities, including effects on cholesterol homeostasis, sphingolipid metabolism, platelet aggregation, apoptosis, and protein prenylation [3–9]. It is also suggested that 24-hydroxycholesterol, 25-hydroxycholesterol, and 27-hydroxycholesterol in serum can be used as a marker of Alzheimer's disease, cerebrotendinous xanthomatosis, Smith-Lemli-Opitz syndrome, and neurodegenerative diseases, respectively [10–15].

In addition, a considerable number of new oxysterols have recently been identified, mainly from patients with a hepatobiliary disease and marine organisms, which contain additional alkyl and/or hydroxy groups at other positions of the C_8*iso*-octane (cholestane) side chain [10–15]. These substituted oxysterols possess an added a chiral center and present the possibility of the appearance in nature of two epimers from the chiral carbon. Thus, the epimers of oxysterols do exist, either individually or as a mixture of the two epimers, in various organisms and the determination of the stereochemistry at a chiral center of oxysterols has been recognized to be important from both biogenetic and phylogenetic viewpoints. Furthermore, oxysterols in biological fluids are of keen current interest in metabolic and catabolic studies. Interest in oxysterols is also due to their physiological function and bioactivity and use as important biomarkers of various human diseases. However, these naturally occurring and specific oxysterols are present only in extremely low concentrations relative to the parent sterols.

As part of a program in our laboratory to synthesize novel and scarce oxysterols that have clinical utility as biomarkers of diseases as well as authentic reference compounds in chromatographic and spectroscopic analysis [16], we report herein the chemical synthesis of 24- and 25-hydroxylated derivatives of 24-alkylsterols epimeric at C-24 and some related compounds and their ^{1}H and ^{13}C NMR characteristics.

Materials and Methods

Materials and Reagents

Campesterol [(24*R*)-24-methyl-cholest-5-en-3β-ol], obtained from Tama Biochemical Co. Ltd., (Tokyo, Japan), was treated with acetic anhydride and pyridine, followed by catalytic hydrogenation of the resulting acetate derivative with a PtO_2 catalyst according to the general procedure to give campestanyl acetate [(24*R*)-24-methyl-5α-cholestan-3β-yl acetate]. Ergostanyl acetate [(24*S*)-24-methyl-5α-cholestan-3β-yl acetate] was from a collection in our laboratory. All other chemicals and solvents were of analytical reagent grade and available from commercial sources.

Instruments

All melting points (mp) were determined on a micro hot-stage apparatus and are uncorrected. NMR spectra were recorded at 23 °C in either $CDCl_3$, C_6D_6 or C_5D_5N by using a JEOL ECA-500 instrument (500.2 MHz for ^{1}H and 125.8 MHz for ^{13}C). Chemical shifts were expressed in δ (ppm) scale, relative to internal Me_4Si and coupling constants (*J*) in Hz. The ^{1}H and ^{13}C resonance assignments were made using a combination of two-dimensional (2D) homonuclear (^{1}H–^{1}H) and heteronuclear (^{1}H–^{13}C) shift-correlated techniques, which include ^{1}H detected heteronuclear multiple quantum correlation (HMQC; ^{1}H–^{13}C coupling) and ^{1}H detected heteronuclear multiple bond correlation (HMBC; long-range ^{1}H–^{13}C coupling) experiments. These 2D-NMR spectra were recorded using standard pulse sequences and parameters recommended by the manufacturer. The ^{13}C distortionless enhancement by polarization transfer (DEPT; 135°, 90°, and 45°) spectra were also measured to determine the exact ^{13}C signal multiplicity and to differentiate between CH_3, CH_2, CH, and C based on their proton environments. High-resolution mass spectra using an electrospray ionization (HR–ESI–MS) were carried out using a JEOL AccuTOF JMS-T100LC liquid chromatograph-mass spectrometer equipped with an ESI source and coupled to an Agilent 1100 series binary pump (Agilent Technologies Inc., Santa Clara, CA, USA) operated in the positive ion mode. The HR-ESI–MS of compounds **2** and **4** were carried out in the flow injection mode, using 10 mM ammonium formate (pH 6.5) and methanol mixture (1:99, v/v) as the mobile phase at a flow rate of 200 µL/min. The ionization conditions were as follows: needle voltage, 2 kV; ion guide peak voltage, 2 kV; ion source temperature, 80 °C; desolvation temperature, 250 °C; orifice voltage, 75 V; mass range, *m/z* 50–1,000; nebulizing gas, N_2 gas. Normal-phase TLC was performed on pre-coated silica gel plates (0.25 mm layer thickness; E. Merck, Darmstadt, Germany) using a mixture of hexane–EtOAc (4:1, v/v) as the developing solvent.

Stereoselective Synthesis of Compounds **2** and **4**

To a magnetically stirred solution of campestanyl acetate (30 mg, 68 µmol) in dry benzene (0.2 mL) and molecular sieves (50 mg, 4 Å), freshly prepared 2,6-dichloropyridine *N*-oxide (DCP) (38 mg, 230 µmol), (5,10,15,20-tetramesitylporphyrinate) ruthenium(II) carbonyl complex [Ru(TMP)CO] (0.3 mg, 0.33 µmol), and HBr (3 µL) were successively added, and the mixture was stirred at 50 °C for 48 h; the reaction was monitored by TLC. After cooling at room temperature, the reaction product was extracted

with toluene, and the combined extract was washed with water, dried with Drierite®, and evaporated to dryness under reduced pressure. The oily product, which consisted of a mixture of two major components by TLC, was chromatographed on a column of silica gel (10 g). Elution with hexane–EtOAc (9:1–8:2, v/v) provided two-well separated fractions.

The less polar fraction was identified as (24*S*)-24-hydroxy-campestanyl acetate (**2**) which crystallized from aqueous methanol as colorless needles; yield, 5.2 mg (17 %); mp, 172–174 °C. High resolution LC–ESI–MS, *m/z* Calc. for $C_{30}H_{53}O_3$ $[M + H]^+$: 461.3995, Found: *m/z* 461.4002.

The more polar fraction was recrystallized from aqueous methanol to give (24*R*)-25-hydroxy-campestanyl acetate (**4**) as colorless needles; yield, 7.6 mg (24 %); mp, 159–160 °C. High resolution LC–ESI–MS, *m/z* Calc. for $C_{30}H_{53}O_3$ $[M + H]^+$: 461.3995, Found: *m/z* 461.4014.

Stereoselective Synthesis of Compounds **1** and **3**

Ergostanyl acetate (500 mg, 1.1 mmol), subjected to the remote-oxidation with Ru(TMP)CO/DCP/HBr and processed as described for the preparation of **2** and **4**, afforded two major products. After chromatographic purification on a column of silica gel, eluting with hexane–EtOAc (9:1–8:2, v/v), gave two well-separated fractions. The less polar component was determined as (24*R*)-24-hydroxy-ergostanyl acetate (**1**) (100 mg, 19 %) and the more polar component as (24*S*)-25-hydroxy-ergostanyl acetate (**3**) (120 mg, 23 %), according to mp, LC–MS, and NMR comparisons with the authentic samples [17, 18].

Results and Discussion

We have recently reported a new stereospecific remote-hydroxylation of a variety of steroids with ethyl(trifluoromethyl)dioxirane [16], dimethyldioxirane [17] or 2,6-dichloropyridine *N*-oxide (DCP) catalyzed by (5,10,15,20-tetramesitylporphrinate) ruthenium(II) carbonyl complex [Ru(TMP)CO] and HBr [18]. The remote *O*-insertion reaction proceeded smoothly, particularly at the hydrogen atom of an unactivated methine carbon (R_3C–H) in the substrates, to give the corresponding hydroxylated derivatives (R_3C–OH) stereoselectively [19, 20]. Alternatively, the stereochemical nature of a newly inserted hydroxy group (e.g., R_3C◄OH) of the oxygenated products was completely retained to that of the hydrogen atom (R_3C◄H) in the starting substrates.

Our initial effort was directed toward stereoselective synthesis of the two C-24 epimer pairs of 24-alkyl oxysterols (**1** vs. **2**; **3** vs. **4**). The starting materials chosen for our synthesis were ergostanyl acetate [tetrahydrobrassicasteryl acetate; (24*S*)-24-methyl-5α-cholestan-3β-yl acetate] and campestanyl acetate [(24*R*)-24-methyl-5α-cholestan-3β-yl acetate], which are derived from ergosterol and campesterol, respectively, by acetylation and subsequent hydrogenation of the resulting acetate derivatives. When the remote *O*-insertion reaction by Ru(TMP)CO/DCP/HBr was subjected to ergostanyl acetate under mild conditions (see Materials and Methods), two major products were isolated after chromatographic purification. Based on the previous findings [17, 18], the two products were identified as (24*R*)-24-hydroxy-ergostanyl acetate [(24*R*)-24-hydroxy-24-methyl-5α-cholestan-3β-yl acetate; **1**] and (24*S*)-25-hydroxy-ergostanyl acetate [(24*S*)-25-hydroxy-24-methyl-5α-cholestan-3β-yl acetate; **3**] without conclusive evidence. In a similar manner, the *O*-insertion reaction of campestanyl acetate with Ru(TMP)CO/DCP/HBr afforded exclusively (24*S*)-24-hydroxy-campestanyl acetate [(24*S*)-24-hydroxy-24-methyl-5α-cholestan-3β-yl acetate; **2**] and (24*R*)-25-hydroxy-campestanyl acetate [(24*R*)-25-hydroxy-24-methyl-5α-cholestan-3β-yl acetate; **4**].

For the purpose of comparison, (24*S*)-24-hydroxy-stigmastanyl acetate [(24*S*)-24-ethyl-24-hydroxy-5α-cholestan-3β-yl acetate; **5**] and (24*R*)-25-hydroxy-stigmastanyl acetate [(24*R*)-24-ethyl-25-hydroxy-5α-cholestan-3β-yl acetate; **6**], prepared in the previous papers [17, 18], were also examined. The chemical structures of stereoisomeric 24-alkyl oxysterol (**1**–**6**) examined in this study are depicted in Fig. 1. These compounds differ from one another in the stereochemical configuration at C-24, the site of hydroxy group (at C-24 or C-25), and/or alkyl substituents (methyl or ethyl at C-24) in the cholestane side chain attached at C-17.

The ^{1}H- and ^{13}C-NMR spectra of sterols and oxysterols and their conjugates (e.g., sulfated derivatives) are conventionally measured in $CDCl_3$ or CD_3OD as a solvent, depending upon their solubility. However, our preliminary work revealed that when (24*S*)-24-hydroxy-campestanyl acetate (**2**) was measured in $CDCl_3$, its 500 MHz ^{1}H-NMR spectrum was unsatisfactory because of the serious CH_3 signal overlapping. To improve ^{1}H and ^{13}C signal resolution, the application of aromatic solvent-induced shift (ASIS) and lanthanide-induced shift (LIS) techniques have been well recognized in previous literatures [21, 22]. Of the two techniques, the ASIS is available in view of the simple procedure, short measuring time, and easy recovery of samples, compared to the LIS. Figure 2 illustrates the ^{1}H-NMR spectra of the compound **2** measured in three variants of the solvent, i.e., $CDCl_3$, C_6D_6, and pyridine-d_6 (C_5D_5N). As can be seen it, the spectral patterns as well as the chemical shifts of each ^{1}H signal were significantly changed by the ASIS effect on the CH_3 signals occurring at upfield region of ca. 0.6–1.4 ppm. Particular noteworthy was that although four CH_3 signals (21-, 26-, 27-, and 28-CH_3) measured in $CDCl_3$ and C_6D_6 solvents are partially

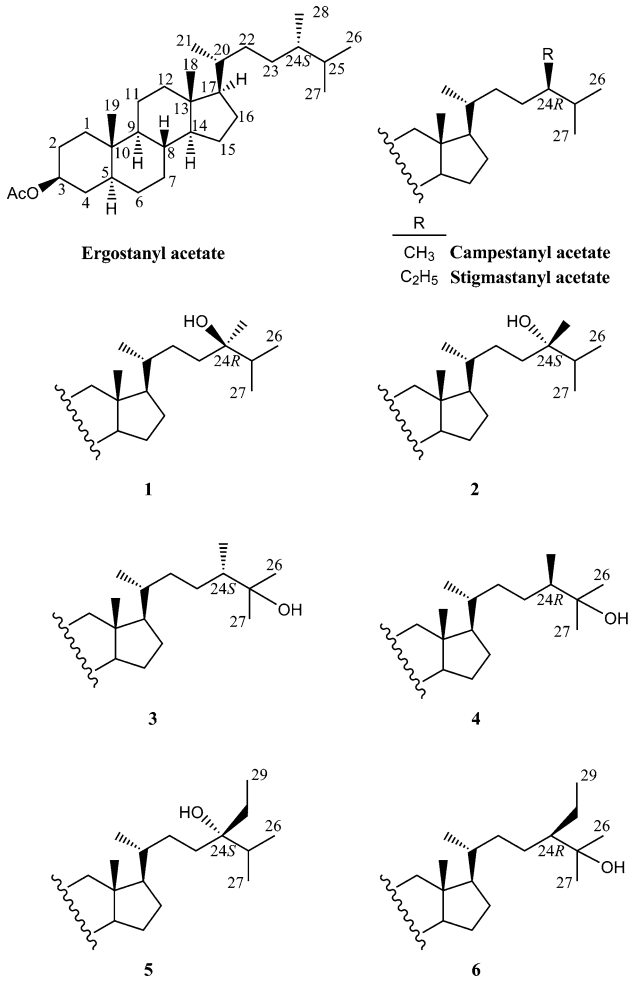

Fig. 1 Chemical structures of 24- and 25-hydroxylated oxysterols (**1**–**6**) examined

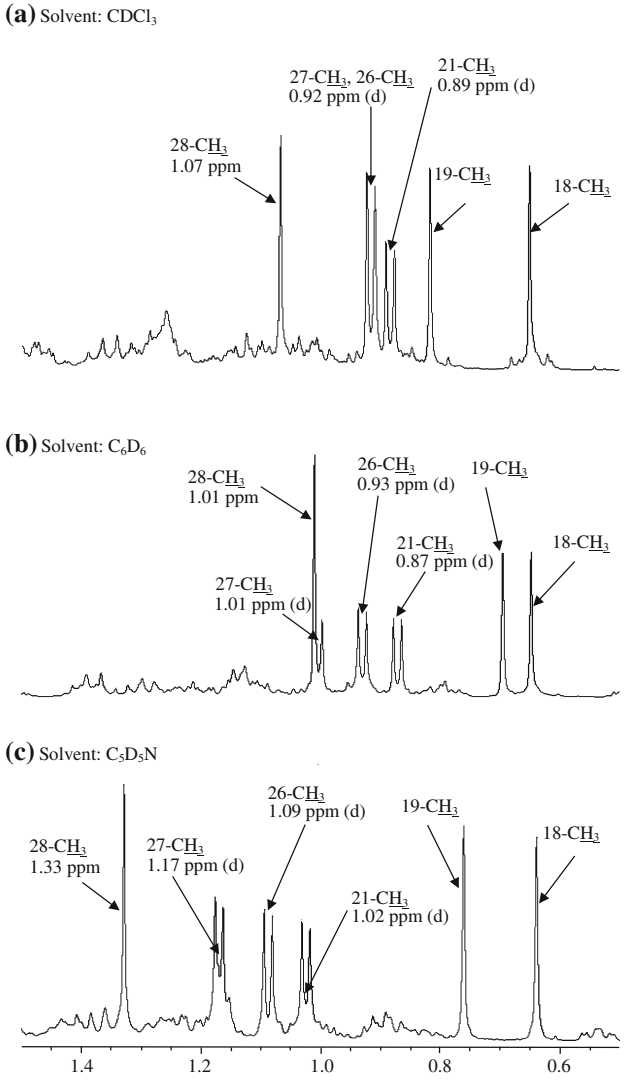

Fig. 2 A part of the ^{1}H-NMR spectra of (24*S*)-24-hydroxy-campestanyl acetate (**2**) measured in **a** $CDCl_3$, **b** C_6D_6, and **c** C_5D_5N

overlapped, these signals are completely resolved from one another in C_5D_5N. Therefore, the use of C_5D_5N seemed to be a more suitable solvent for measuring this type of 24-alkyl oxysterols.

Table 1 compiles the ^{1}H and ^{13}C chemical shift data for the compound **2** measured in $CDCl_3$, C_6D_6, and C_5D_5N solvents. The ^{13}C signal assignments were made exclusively by the use of the DEPT spectra. 2D heteronuclear (^{1}H–^{13}C) shift-correlated HMQC and HMBC techniques were also used to further confirm the ^{1}H and ^{13}C correlations, as shown in Fig. 3. The differences in the ^{1}H and ^{13}C chemical shift (δ_H and δ_C) values of the substrate measured in $CDCl_3$ vs. C_5D_5N (or $CDCl_3$ vs. C_6D_6) were expressed in terms of the ASIS $^{H}\Delta\delta$- and $^{C}\Delta\delta$-values, respectively; the negative and positive values show the down-field and up-field shifts, respectively, relative to the δ_H (or δ_C) values measured in $CDCl_3$.

Based on the above findings, the δ_H and δ_C values and signal multiplicities for all of the six 24-alkyl oxysterols (**1**–**6**) measured in C_5D_5N are compiled in Table 2. In analogy with the ASIS $^{H}\Delta\delta$- and $^{C}\Delta\delta$-values mentioned above, the epimeric $^{H}\Delta\delta$- and $^{C}\Delta\delta$-values represent the differences in the δ_H and δ_C values in two C-24 epimeric pairs of 24-methyl oxysterols: i.e., **1** vs. **2**; **3** vs. **4**.

A large number of the ^{1}H- and ^{13}C-NMR data of steroids as well as sterols have been reviewed by Kirk et al. [23], Blunt and Stothers [24], and Goad and Akihisa [25, 26]. According to the previous observation by Rubinstein et al. [27], eight pairs of epimeric 24-alkylsterols could be distinguished by 220 MHz ^{1}H-NMR spectra. Similarly, identification of six pairs of epimeric 24-alkylsterols was attained at 25.16 MHz ^{13}C NMR by Wright et al. [28].

As shown in Fig. 4, when a pair of C-24 epimeric (24*R*)-24-hydroxy-ergostanyl acetate (**1**) and (24*S*)-24-hydroxy-campestanyl acetate (**2**) were measured in C_5D_5N, both the epimers exhibited essentially identical ^{1}H-NMR spectra

Table 1 ^{1}H- and ^{13}C-NMR chemical shifts for (24*S*)-24-hydroxy-campestanyl acetate (**2**) measured in different solvents

Carbon no	Type	$CDCl_3$		C_6D_6		ASIS$^{H}\Delta\delta$- and$^{C}\Delta\delta$-values		C_5D_5N		ASIS$^{H}\Delta\delta$- and$^{C}\Delta\delta$-values	
		^{13}C	^{1}H	^{13}C	^{1}H	^{13}C	^{1}H	^{13}C	^{1}H	^{13}C	^{1}H
1	CH_2	36.74		36.90		−0.16		36.84[a]		−0.10	
2	CH_2	27.46		27.94		−0.48		27.81		−0.35	
3	CH	73.77	4.68 (m)	73.49	4.89 (m)	0.28	−0.21	73.69	4.86 (m)	0.08	−0.18
4	CH_2	34.01		34.50		−0.49		34.34		−0.33	
5	CH	44.64		44.66		−0.02		44.67		−0.03	
6	CH_2	28.58		28.84		−0.26		28.77		−0.19	
7	CH	31.96		32.22		−0.26		32.13		−0.17	
8	CH	35.44		35.65		−0.21		35.52		−0.08	
9	CH	54.19		54.30		−0.11		54.25		−0.06	
10	C	35.44		35.53		−0.09		35.52		−0.08	
11	CH_2	21.17		21.47		−0.30		21.40		−0.23	
12	CH	39.94		40.33		−0.39		40.14		−0.20	
13	C	42.59		42.83		−0.24		42.74		−0.15	
14	CH	56.38		56.62		−0.24		56.46		−0.08	
15	CH_2	24.18		24.51		−0.33		24.39		−0.21	
16	CH_2	28.21		28.59		−0.38		28.51		−0.30	
17	CH	55.95		56.41		−0.46		56.38		−0.43	
18	CH_3	12.06	0.65 (s)	12.22	0.65 (s)	−0.16	0.00	12.22	0.64 (s)	−0.16	0.01
19	CH_3	12.21	0.82 (s)	12.30	0.70 (s)	−0.09	0.12	12.24	0.76 (s)	−0.03	0.06
20	CH	36.13		36.57		−0.44		36.61		−0.48	
21	CH_3	18.74	0.89 (d, 6.9)	19.07	0.87 (d, 6.9)	−0.33	0.02	19.09	1.02 (d, 6.9)	−0.35	−0.13
22	CH_2	29.14		29.57		−0.43		29.78		−0.64	
23	CH_2	35.96		36.47		−0.51		36.83[a]		−0.87	
24	C	74.79		74.08		0.71		73.57		1.22	
25	CH	36.59		36.99		−0.40		37.37		−0.78	
26	CH_3	17.48	0.92 (d, 6.9)	17.68	0.93 (d, 6.9)	−0.20	−0.01	18.02	1.09 (d, 6.9)	−0.54	−0.17
27	CH_3	16.94	0.92 (d, 6.9)	17.16	1.01 (d, 6.3)	−0.22	−0.09	17.61	1.17 (d, 6.9)	−0.67	−0.25
28	CH_3	23.32	1.07 (s)	23.58	1.01 (s)	−0.26	0.06	23.85	1.33 (s)	−0.53	−0.26
$O\underline{C}OCH_3$	C	170.71		169.70		1.01		170.30		0.41	
$OCO\underline{C}H_3$	CH_3	21.48	2.02 (s)	21.06	1.77 (s)	0.42	0.25	21.31	2.07 (s)	0.17	−0.05

The difference in the chemical shifts between the substrate measured in two different solvents

[a] Assignments along a vertical column may be interchanged

and were indistinguishable from each other. However, a careful comparison of **1** and **2** revealed that small, but distinct differences for characterizing each epimer are detected in the ^{13}C-NMR spectra. Thus, the ^{13}C signals arising from the C-23 and C-25 in **1** resonated at 37.11 and 36.79 ppm, respectively, while the corresponding signals in **2** appeared at 36.83 and 37.37 ppm, respectively: the epimeric $^{C}\Delta\delta$-values observed are 0.28 and −0.59 ppm. The δ_C differences should therefore be utilized to characterize each of the two epimers, except for the C-26 and C-27 ^{1}H and ^{13}C resonances (see below).

A similar relationship was also observed between a pair of C-24 epimeric (24*S*)-25-hydroxy-ergostanyl acetate (**3**) and (24*R*)-25-hydroxy-campestanyl acetate (**4**). As shown in Fig. 5, there is no significant difference in the ^{1}H-NMR spectra of **3** and **4**, but significant features to characterize the individual epimers were observed on the ^{13}C-NMR spectra. Those were the ^{13}C signals arising from the C-20–C-22 and C-28; the epimeric $^{C}\Delta\delta$-values observed were 0.42–0.57 ppm. Of further importance was that a more diagnostic, large difference is detected for the epimeric $^{C}\Delta\delta$-value (0.85 ppm) for the chiral carbon itself at C-24.

In the ^{1}H-NMR spectrum of (24*S*)-24-hydroxy-stigmastanyl acetate (**5**), one triplet signal appearing at 1.07 ppm and two doublet signals occurring at 1.13 and 1.15 ppm

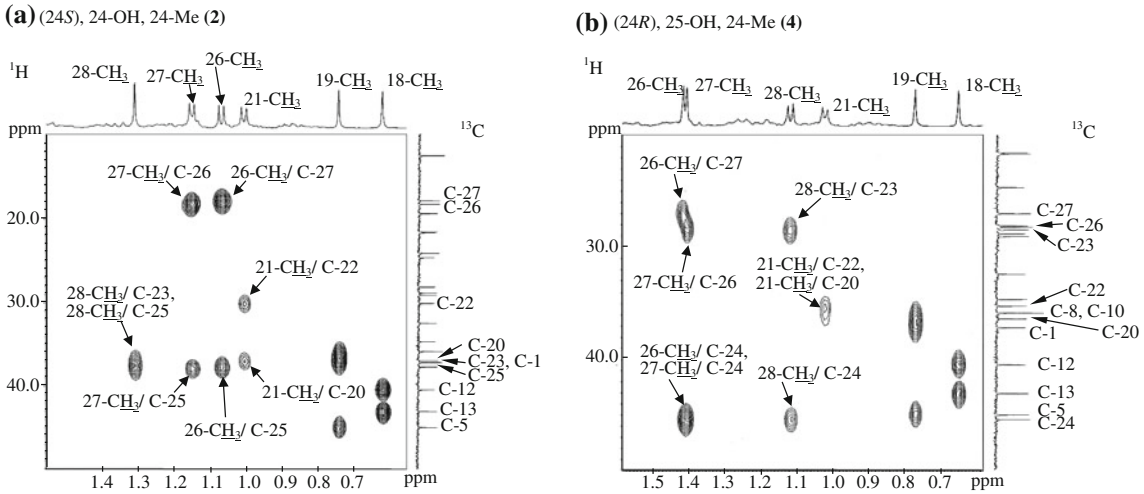

Fig. 3 A part of the HMBC spectra of **a** (24*S*)-24-hydroxy-campestanyl acetate (**2**) and **b** (24*R*)-25-hydroxy-campestanyl acetate (**4**)

were assigned to the 29-CH_3 and the 26- and 27-CH_3 signals, respectively. The remaining 18-, 19-, and 21-CH_3 signals in **5** showed the same chemical shifts to those observed in (24*S*)-24-hydroxy-campestanyl acetate (**2**), probably because **2** and **5** differ only the alkyl substituent at C-24. In addition, the ^{13}C-NMR spectra of the two compounds differed remarkably from each other, particularly in the δ_C values of the C-23, C-24, C-25, and C-28 signals, due to the α- and β-effects of a different length of the alkyl substituents (see Table 2).

Analogously, predominant α-, β- and γ-shifts of the neighboring ^{13}C signals were also observed between (24*R*)-25-hydroxy-stigmastanyl acetate (**6**) and (24*R*)-25-hydroxy-campestanyl acetate (**4**).

There is considerable uncertainty in the literature [25, 26] on the ^{1}H and ^{13}C assignments of the terminal isopropyl methyl (26-/27-CH_3) signals. The cholestrane side chain without a substituent affords the 26-/27-CH_3 ^{1}H signals at 0.85–0.89 ppm as equivalent doublets, because both the CH_3 groups are chemically equivalent by the free rotation of the σ-bond between the C-24 and C-25. On the other hand, the two 26-/27-CH_3 signals in alkylsterol and oxysterols having a substituent in the side chain render nonequivalent and usually show different δ_H values. In analogy with the 26-/27-CH_3, the C-26/C-27 ^{13}C signals in these compounds are also nonequivalent. In the case of the compounds **1**–**6** examined in this study, the major reason for the nonequivalence of the 26-/27-CH_3 ^{1}H signals arises from a combined effect of the inductive effect and steric interaction of the substituents (i.e., CH_3 and OH groups), whereas that of the C-26/C-27 ^{13}C signals principally suffers non-bonded interaction so-called "gauche γ-substituent effect" [24, 29, 30].

Figure 6 shows Newman's projection formula for the most preferred conformation of compounds **1**–**4**. Assuming that the 24-OH in the (24*R*)-24-hydroxy compound (**1**) is antiperiplanar with respect to the 27-CH_3, the electron-donating 26-CH_3 which has a gauche arrangement may be more effectively shifted to down-field (deshielding) by the inductive effect of the electron-withdrawing 24-OH: thereby 26-CH_3 ^{1}H signal (doublet) resonates at 1.17 ppm and the 27-CH_3 at 1.08 ppm. Meanwhile, differentiation between the C-26/C-27 ^{13}C signals in **1** was basically made on the gauche γ-substituent effect. Thus, both the C-26/C-27 are situated in the γ-position with respect to the C-24 bearing the 24-OH. The conformational arrangement of the 24-OH vs. 26-CH_3 is gauche, while that of the 24-OH vs. 27-CH_3 is anti. These facts suggest that shift to up-field (shielding) caused by gauche γ-substituent is much more pronounced for the C-26 than for the 27-CH_3. Thus, the ^{13}C signal appearing at up-field of 17.51 ppm was assigned to the C-26 and the other one occurring at down-field of 18.09 ppm to the C-27. The validity of the above tentative ^{1}H and ^{13}C assignments in **1** was further confirmed by measuring the 2D HMQC and HMBC spectra (Fig. 3).

On the other hand, the reverse relationship is true for the (24*S*)-hydroxy epimer (**2**): the 26-CH_3 (1.09 ppm) ^{1}H signal resonates at higher-field than the 27-CH_3 (1.17 ppm). Based on the ^{1}H signal assignments, the corresponding C-26/C-27 ^{13}C signals were directly correlated by the HMQC and HMBC spectra. The result exhibited that the ^{13}C signals occurring at 18.02 and 17.61 ppm in **2** were assigned to the C-26 and C-27, respectively.

Meanwhile, if the 25-OH and 23-CH_2- in (24*S*)-25-hydroxy compound (**3**) has antiperiplanar conformation, shift to up-field by the inductive effect of the 28-CH_3 on the gauche 26-CH_3 seems to be slightly effective, compared to that on the anti 27-CH_3. The CH_3 ^{1}H signal (singlet) occurring at 1.39 ppm was therefore assigned to the 26-CH_3 and the other one appearing at 1.41 ppm to the

Table 2 ^{1}H- and ^{13}C chemical shifts for compounds **1–6** measured in C_5D_5N

Carbon no	Type	**1**		**2**		Epimeric $^{H}\Delta\delta$- and $^{C}\Delta\delta$-values[a]	
		^{13}C	^{1}H	^{13}C	^{1}H	^{13}C	^{1}H
1	CH_2	36.84		36.84[b]		0.00	
2	CH_2	27.80		27.81		−0.01	
3	CH	73.69	4.86 (m)	73.69	4.86 (m)	0.00	0.00
4	CH_2	34.34		34.34		0.00	
5	CH	44.67		44.67		0.00	
6	CH_2	28.77		28.77		0.00	
7	CH	32.13		32.13		0.00	
8	CH	35.53		35.52		0.01	
9	CH	54.25		54.25		0.00	
10	C	35.53		35.52		0.01	
11	CH_2	21.41		21.40		0.01	
12	CH	40.14		40.14		0.00	
13	C	42.74		42.74		0.00	
14	CH	56.47		56.46		0.01	
15	CH_2	24.40		24.39		0.01	
16	CH_2	28.53		28.51		0.02	
17	CH	56.32		56.38		−0.06	
18	CH_3	12.22	0.65 (s)	12.22	0.64 (s)	0.00	0.01
19	CH_3	12.24	0.76 (s)	12.24	0.76 (s)	0.00	0.00
20	CH	36.55		36.61		−0.06	
21	CH_3	19.09	1.02 (d, 6.9)	19.09	1.02 (d, 6.9)	0.00	0.00
22	CH_2	29.72		29.78		−0.06	
23	CH_2	37.11		36.83[b]		0.28	
24	C	73.55		73.57		−0.02	
25	CH	36.79		37.37		−0.58	
26	CH_3	17.51	1.17 (d, 6.9)	18.02	1.09 (d, 6.9)	−0.51	0.08
27	CH_3	18.09	1.08 (d, 6.9)	17.61	1.17 (d, 6.9)	0.48	−0.09
28	CH_3	23.84	1.32 (s)	23.85	1.33 (s)	−0.01	−0.01
$O\underline{C}OCH_3$	C	170.30		170.30		0.00	
$OCO\underline{C}H_3$	CH_3	21.31	2.07 (s)	21.31	2.07 (s)	0.00	0.00
Carbon no	Type	**3**		**4**		Epimeric $^{H}\Delta\delta$- and $^{C}\Delta\delta$-values	
		^{13}C	^{1}H	^{13}C	^{1}H	^{13}C	^{1}H
1	CH_2	36.86		36.84		0.02	
2	CH_2	27.82		27.81		0.01	
3	CH	73.70	4.86 (m)	73.69	4.86 (m)	0.01	0.00
4	CH_2	34.35		34.35		0.00	
5	CH	44.69		44.67		0.02	
6	CH_2	28.78		28.77		0.01	
7	CH	32.15		32.15		0.00	
8	CH	35.56		35.55		0.01	
9	CH	54.28		54.26		0.02	
10	C	35.56		35.53		0.03	
11	CH_2	21.41		21.41		0.00	
12	CH	40.13		40.17		−0.04	
13	C	42.72		42.76		−0.04	
14	CH	56.41		56.47		−0.06	

Table 2 continued

Carbon no	Type	**3**		**4**		Epimeric $^{H}\Delta\delta$- and $^{C}\Delta\delta$-values	
		^{13}C	^{1}H	^{13}C	^{1}H	^{13}C	^{1}H
15	CH_2	24.41		24.41		0.00	
16	CH_2	28.46		28.55		−0.09	
17	CH	56.17		56.47		−0.30	
18	CH_3	12.23	0.65 (s)	12.22	0.64 (s)	0.01	0.01
19	CH_3	12.24	0.76 (s)	12.24	0.76 (s)	0.00	0.00
20	CH	36.64		36.07		0.57	
21	CH_3	19.27	1.02 (d, 6.9)	18.85	1.02 (d, 6.9)	0.42	0.00
22	CH_2	35.42		34.92		0.50	
23	CH_2	28.22		28.17		0.05	
24	CH	45.95		45.10		0.85	
25	C	72.21		72.12		0.09	
26	CH_3	26.46	1.39 (s)	27.95	1.41 (s)	−1.49	−0.02
27	CH_3	28.18	1.41 (s)	26.71	1.39 (s)	1.47	0.02
28	CH_3	15.42	1.12 (d, 6.9)	14.93	1.12 (d, 6.9)	0.49	0.00
$O\underline{C}OCH_3$	C	170.30		170.30		0.00	
$OCO\underline{C}H_3$	CH_3	21.32	2.07 (s)	21.31	2.07 (s)	0.01	0.00

Carbon no	Type	**5**		**6**	
		^{13}C	^{1}H	^{13}C	^{1}H
1	CH_2	36.87		36.85	
2	CH_2	27.83		27.82	
3	CH	73.70	4.86 (m)	73.70	4.86 (m)
4	CH_2	34.36		34.35	
5	CH	44.68		44.68	
6	CH_2	28.79		28.78	
7	CH	32.15		32.16	
8	CH	35.55		35.56	
9	CH	54.26		54.27	
10	C	35.57		35.56	
11	CH_2	21.43		21.43	
12	CH	40.17		40.18	
13	C	42.78		42.77	
14	CH	56.49		56.51	
15	CH_2	24.43		24.43	
16	CH_2	28.60		28.60	
17	CH	56.46		56.33	
18	CH_3	12.24	0.64 (s)	12.24	0.65 (s)
19	CH_3	12.24	0.76 (s)	12.24	0.76 (s)
20	CH	36.93		36.64	
21	CH_3	19.11	1.03 (d, 6.3)	19.00	1.05 (d, 6.3)
22	CH_2	29.70		36.39	
23	CH_2	32.58		27.48	
24	C	75.01		52.47	
25	CH	34.63		72.74	
26	CH_3	17.46	1.13 (d, 5.2)	28.11	1.42 (s)
27	CH_3	17.33	1.15 (d, 5.2)	28.00	1.42 (s)
28	CH_2	29.06		24.20	

Table 2 continued

Carbon no	Type	**5**		**6**	
		^{13}C	^{1}H	^{13}C	^{1}H
29	CH_3	8.35	1.07 (t, 7.4)	14.51	1.12 (t, 7.2)
$O\underline{C}OCH_3$	C	170.30		170.30	
$OCO\underline{C}H_3$	CH_3	21.33	2.07 (s)	21.31	2.07 (s)

[a] The difference in the ^{1}H or ^{13}C chemical shifts between an epimeric pair of the substrates

[b] Assignments along a vertical column may be interchanged

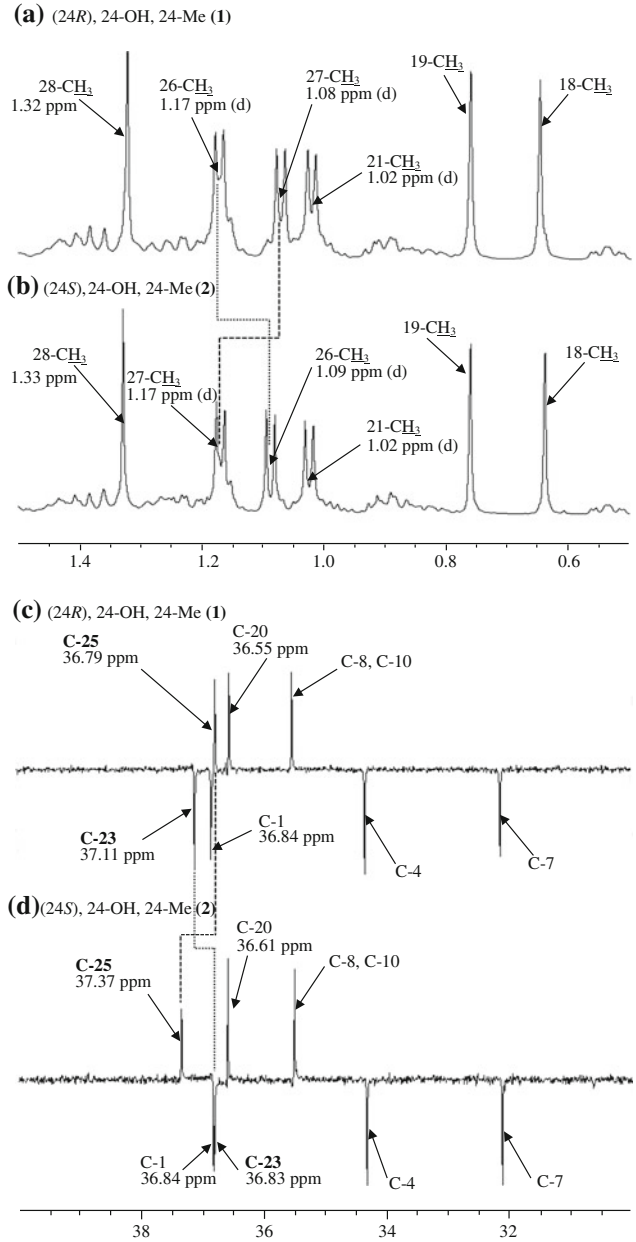

Fig. 4 A part of the ^{1}H-NMR spectra of **a** (24*R*)-24-hydroxy-ergostanyl acetate (**1**) and **b** (24*S*)-24-hydroxy-campestanyl acetate (**2**) and their ^{13}C NMR DEPT spectra [**c** and **d**] measured in C_5D_5N

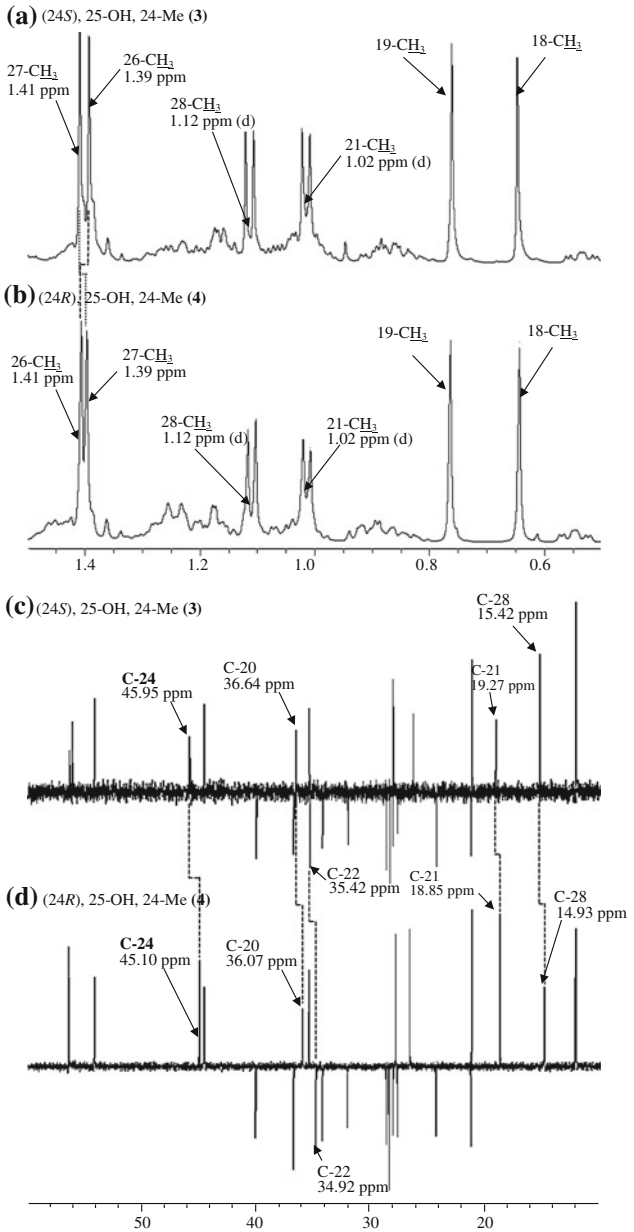

Fig. 5 A part of the ^{1}H-NMR spectra of **a** (24*S*)-25-hydroxy-ergostanyl acetate (**3**) and **b** (24*R*)-25-hydroxy-campestanyl acetate (**4**) and their ^{13}C-NMR DEPT spectra [**c** and **d**] measured in C_5D_5N

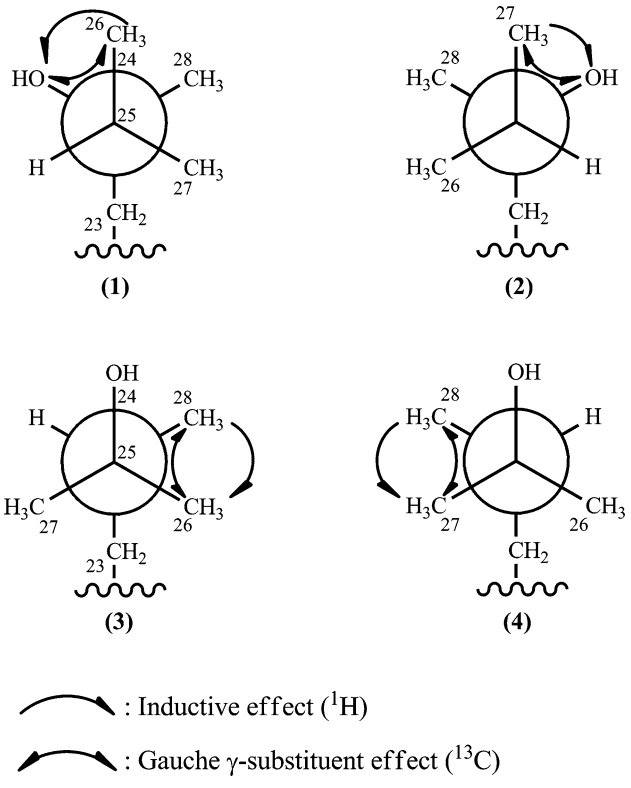

Fig. 6 Newman's projection formula for the preferred conformation of compounds **1**–**4**

27-CH_3. In addition, up-field shift by the gauche γ-substituent effect of the 28-CH_3 on the C-26 in **3** is more efficient than that on the C-27, indicating that the ^{13}C signal at 26.46 ppm is assigned to the C-26 and at 28.18 ppm to the C-27. The reverse is also true for the (24*R*)-25-hydroxy epimer (**4**): the ^{1}H signals at 1.41 ppm was assigned to the 26-CH_3 and at 1.39 ppm to the 27-CH_3; the^{13}C signal of the C-26 and C-27 are assigned to 27.95 and 26.71 ppm, respectively. The tentative assignments were confirmed by measuring the respective HMQC and HMBC spectra.

In (24*S*)-24-hydroxy-stigmastanyl acetate (**5**) and (24*R*)-25-hydroxy-stigmastanyl acetate (**6**) with an ethyl group at C-24, their 26-/27-CH_3 ^{1}H and C-26/C-27 ^{13}C signal assignments were carried out on the basis of the corresponding 24- and 25-hydroxylated derivatives of campestanyl acetates (**2** and **4**), respectively. Particular attention should therefore be paid for the two isopropyl methyl assignments in oxysterols with an additional substituent in the cholestane side chain, because only the use of the δ_H- and δc-values are difficult to characterize each of the (24*R*)/(24*S*)-diastereomers. Additional confirmation of the two isopropyl methyl assignments of 24-alkyl oxysterol epimers by their deuterium labeled derivatives at C-26 or C-27 is desirable.

In conclusion, the ASIS by C_5D_5N was recommended as a suitable solvent to determine the (24*R*)-/(24*S*)-configuration of epimeric 24-alkyl oxysterols. Differentiation between two epimeric pairs of the 24- and 25-hydroxylated derivatives of 24-alkylsterols was particularly achieved by the ^{13}C-NMR measurement in C_5D_5N. Studies of the natural occurrence of 24-alkyl oxysterols and their biological and physiological importance as well as their use as biomarkers of human diseases are now progressing in our laboratory. Availability of the synthetic 24-alkyl oxysterols as authentic reference compounds may also be useful for their identification and analysis in biological materials. A further detailed study is now progressing in our laboratory, and the result will be reported at a later date.

Acknowledgments This work was supported in part by a Grant-in-Aid for Scientific Research from the Ministry of Education, Culture, Sports, Sciences and Technology of Japan (to T.I., 24550107) for 2012–2014 and for the Strategic Research Base Development Program for Private Universities subsidized MEXT 2009 (S0901022) for 2009–2013.

References

1. Akihisa T, Kokke W (1991) Naturally occurring sterols and related compounds from plants In: Patterson GW, Nes WD (eds) Physiology and biochemistry of sterols. AOCS press, Champaign
2. Derdemezis CS, Filippatos TD, Mikhailidis DP, Elisaf MS (2010) Effects of plant sterols and stanols beyond low-density lipoprotein cholesterol lowering. J Cardiovasc Pharmacol Ther 15:120–134
3. Lund EG, Guileyardo JM, Russell DW (1999) cDNA cloning of cholesterol 24-hydroxylase, a mediator of cholesterol homeostasis in the brain. Proc Natl Acad Sci USA 96:7238–7243
4. Ren S, Hylemon P, Zhang ZP, Rodriguez-Agudo D, Marques D, Li X, Zhou H, Gil G, Pandak WM (2006) Identification of a novel sulfonated oxysterol, 5-cholesten-3β,25-diol 3-sulfonate, in hepatocyte nuclei and mitochondria. J Lipid Res 47:1081–1090
5. Ren S, Li X, Rodriguez-Agudo D, Gil G, Hylemon P, Pandak WM (2007) Sulfated oxysterol, 25HC3S, is a potent regulator of lipid metabolism in human hepatocytes. Biochem Biophys Res Commun 360:802–808
6. Liu C, Yang XV, Wu J, Kuei C, Mani NS, Zhang L, Yu J, Sutton SW, Qin N, Banie H, Karlsson L, Sun S, Lovenberg TW (2011) Oxysterols direct B-cell migration through EBI2. Nature 475:519–523
7. Hannedouche S, Zhang J, Yi T, Shen W, Nguyen D, Pereira JP, Guerini D, Baumgarten BU, Roggo S, Wen B, Knochenmuss R, Noel S, Gessier F, Kelly LM, Vanek M, Laurent S, Preuss I, Miault C, Christen I, Karuna R, Li W, Koo DI, Suply T, Schmedt C, Peters EC, Falchetto R, Katopodis A, Spanka C, Roy MO, Detheux M, Chen YA, Schultz PG, Cho CY, Seuwen K, Cyster JG, Sailer AW (2011) Oxysterols direct immune cell migration via EBI2. Nature 475:524–527
8. Bjorkhem I (2002) Do oxysterols control cholesterol homeostasis? J Clin Invest 110:725–730
9. Fourgeux C, Bron A, Acar N, Creuzot-Garcher C, Bretillon L (2011) 24S-Hydroxycholesterol and cholesterol-24S-hydroxylase (CYP46A1) in the retina: from cholesterol homeostasis to pathophysiology of glaucoma. Chem Phys Lipids 164:496–499

10. Cali JJ, Hsieh CL, Francke U, Russell DW (1991) Mutations in the bile acid biosynthetic enzyme sterol 27-hydroxylase underlie cerebrotendinous xanthomatosis. J Biol Chem 266:7779–7783
11. Russell DW (2000) Oxysterol biosynthetic enzymes. Biochim Biophys Acta 1529:126–135
12. Kanebratt KP, Diczfalusy U, Backstrom T, Sparve E, Bredberg E, Bottiger Y, Andersson TB, Bertilsson L (2008) Cytochrome P450 induction by rifampicin in healthy subjects: determination using the Karolinska cocktail and the endogenous CYP3A4 marker 4β-hydroxycholesterol. Clin Pharmacol Ther 84:589–594
13. Xu L, Korade Z, Rosado DA Jr, Liu W, Lamberson CR, Porter NA (2011) An oxysterol biomarker for 7-dehydrocholesterol oxidation in cell/mouse models for Smith-Lemli-Opitz syndrome. J Lipid Res 52:1222–1233
14. Leoni V, Caccia C (2011) Oxysterols as biomarkers in neurodegenerative diseases. Chem Phys Lipids 164:515–524
15. Wolozin B (2003) Cyp46 (24S-cholesterol hydroxylase): a genetic risk factor for Alzheimer disease. Arch Neurol 60:16–18
16. Ogawa S, Kakiyama G, Muto A, Hosoda A, Mitamura K, Ikegawa S, Hofmann AF, Iida T (2009) A facile synthesis of C-24 and C-25 oxysterols by in situ generated ethyl(trifluoromethyl)dioxirane. Steroids 74:81–87
17. Iida T, Yamaguchi T, Nakamori R, Hikosaka M, Mano N, Goto J, Nambara T (2001) A highly efficient, stereoselective oxyfunctionalization of unactivated carbons in steroids with dimethyldioxirane. J Chem Soc Perkin Trans 1:2229–2236
18. Iida T, Ogawa S, Miyata S, Goto T, Mano N, Goto J, Nambara T (2004) Biomimetic oxidation of unactivated carbons in steroids by a model of cytochrome P-450, oxorutheniumporphyrinate complex. Lipids 39:873–880
19. Ohtake H, Higuchi T, Hirobe M (1992) Highly efficient oxidation of alkanes and alkyl alcohols with heteroaromatic N-oxides catalyzed by ruthenium porphyrins. J Am Chem Soc 114:10660–10662
20. Shingaki T, Miura K, Higuchi T, Hirobe M, Nagano T (1997) Regio- and stereo-selective oxidation of steroids using 2,6-dichloropyridine N-oxide catalysed by ruthenium porphyrins. Chem Commun 861–862
21. Iida T, Kikuchi M, Tamura T, Matsumoto T (1977) Lanthanide and aromatic solvent-induced shift effects on proton resonances in C-4-methylated steroids and tetracyclic triterpenoids. Chem Phys Lipids 20:157–174
22. Iida T, Tamura T, Matsumoto T (1980) Proton nuclear magnetic resonance identification and discrimination of side chain isomers of phytosterols using a lanthanide shift reagent. J Lipid Res 21:326–338
23. Kirk DN, Toms HC, Douglas C, White KA, Smith KE, Latif S, Hubbard RWP (1990) A survey of the high-field ^{1}H NMR spectra of the steroid hormones, their hydroxylated derivatives, and related compounds. J Chem Soc Perkin Trans 2:1567–1594
24. Blunt JW, Stothers JB (1977) ^{13}C n.m.r. spectra of steroids—a survey and commentary. Org Magn Reson 9:439–464
25. Goad LJ, Akihisa T (1997) ^{1}H NMR spectroscopy of sterols. In: Analysis of sterols, chap 8. Blackie Academic & Professional, London, pp 197–234
26. Goad LJ, Akihisa T (1997) ^{13}C NMR spectroscopy of sterols. In: Analysis of sterols, chap 9. Blackie Academic & Professional, London, pp 235–255
27. Rubinstein I, Goad LJ, Clague ADH, Mulheirn LJ (1976) The 220 MHz NMR spectra of phytosterols. Phytochem 15:195–200
28. Wright JLC, McInnes AG, Shimizu S, Smith DG, Walter JA, Idler D, Khalil W (1978) Identification of C-24 alkyl epimers of marine sterols by ^{13}C nuclear magnetic resonance spectroscopy. Can J Chem 56:1898–1903
29. Beierbeck H, Saunders JK (1976) A reinterpretation of beta, gamma, and delta substituent effects on ^{13}C chemical shifts. Can J Chem 54:2985–2995
30. Schwenzer GM (1978) Analysis of carbon-13 nuclear magnetic resonance for monohydroxy steroids incorporating geometric distortions. J Org Chem 43:1079–1083